Volume 11, Issue 7, July – 2026 International Journal of Innovative Science and Research Technology
ISSN No:-2456-2165 https://doi.org/10.38124/ijisrt/26jul1280

Metaheuristically Optimized ViT–DBN Diagnostic Model for Early Alzheimer's Disease Detection

Annappa S. S.[1]; Asha S.[2]; Lohith C.[3]

[1]Guest Lecturer, Department of Computer Science, Sahyadri Science College, Shimoga, India
[2]Guest Lecturer, Department of Computer Science, Sahyadri Science College, Shimoga, India
[3]Assistant Professor, Department CSE (IoT & CSBT), East Point College of Engineering and Technology, Bengaluru, India

Publication Date: 2026/07/28

Abstract: Timely and effective treatment of Alzheimer's disease (AD) depends heavily on early detection. This work proposes a hybrid Vision Transformer (ViT) and Deep Belief Network (DBN) model, metaheuristically optimized for early AD detection from brain MRI images. Prior to classification, an Adaptive Cancellation Filter (ACF) is applied to eliminate noise and enhance structural features. The DBN–ViT architecture enables effective hierarchical feature learning while jointly capturing long-range and local dependencies within the imaging data. To improve convergence and stability, the Chimp Optimization Algorithm (ChOA) is used to optimize the model's parameters. Experimental results show that the proposed model outperforms Convolutional Neural Network (92%) and Decision Tree (89%) techniques, achieving 95% accuracy, precision, recall, and F1-score, indicating strong robustness and clinical applicability.

Keywords: *Vision Transformer (ViT); Deep Belief Network (DBN); Adaptive Cancellation Filter (ACF); Chimp Optimization Algorithm (ChOA).*

How to Cite: Annappa S. S.; Asha S.; Lohith C. (2026) Metaheuristically Optimized ViT–DBN Diagnostic Model for Early Alzheimer's Disease Detection. *International Journal of Innovative Science and Research Technology*, 11(7), 1410-1417. https://doi.org/10.38124/ijisrt/26jul1280

I. INTRODUCTION

Alzheimer's disease (AD) is a progressive neurodegenerative disorder and the most common cause of dementia worldwide. It impairs memory, cognitive ability, and behaviour. As the global elderly population continues to grow, the incidence of AD is rising sharply, with significant implications for public health. Early diagnosis is often missed because the initial symptoms of AD are difficult to distinguish from normal age-related decline. Timely identification allows healthcare professionals to intervene earlier and manage the disease more effectively, thereby improving patient outcomes and overall quality of life.

AD is a complex, multi-factorial condition arising from the interaction of genetic, environmental, epigenetic, and metabolic factors. This interaction produces considerable variability in the cognitive symptoms experienced by different individuals. Owing to this complexity, the development of effective treatments has progressed slowly, as reflected in the high attrition rate of drug candidates throughout the AD clinical trial process.

Accurate AD diagnosis from medical imaging depends heavily on effective preprocessing. Gaussian smoothing is a simple and fast method for reducing MRI noise, but it tends to blur fine details that are essential for early detection [5]. Median filtering removes noise by estimating pixel values from neighbouring pixels and preserves edges reasonably well, but like Gaussian smoothing, it can distort small structural details [6]. The Adaptive Cancellation Filter (ACF), in contrast, dynamically adjusts its filter parameters to suppress noise while retaining features relevant to diagnosis.

Feature extraction is equally critical for identifying meaningful patterns in neuroimaging data. The Discrete Wavelet Transform (DWT) decomposes signals for compression and noise reduction but is computationally complex and can result in information loss [7]. The Grey-Level Co-occurrence Matrix (GLCM) extracts texture information by analysing pixel-intensity relationships, but it is computationally intensive and sensitive to noise [8]. The proposed DBN–ViT combination addresses these limitations by jointly strengthening feature learning and classification accuracy.

Optimization techniques further improve deep learning models by increasing accuracy and accelerating convergence. Genetic Algorithms (GA) optimize models through selection, crossover, and mutation but converge slowly and demand substantial computation [9]. Particle Swarm Optimization

ISSN No:-2456-2165 https://doi.org/10.38124/ijisrt/26jul1280

(PSO) relies on personal and global best positions but tends to converge prematurely in complex search spaces [10]. The Chimp Optimization Algorithm (ChOA) instead mimics chimpanzee hunting behaviour to balance exploration and exploitation efficiently while searching for optimal solutions.

Taken together, the proposed metaheuristically optimized ViT–DBN model offers a reliable and effective diagnostic tool for AD, supporting improved clinical decision-making.

➢ *Objectives*

- To reduce noise and preserve important anatomical detail in MRI images using an ACF.
- To partition the preprocessed data into training and testing sets for balanced model learning and evaluation.
- To extract discriminative characteristics from brain images using a DBN.
- To capture both local and global patterns in imaging data using the ViT attention mechanism.
- To improve the accuracy and convergence of the DBN–ViT model parameters using ChOA.
- To classify images into AD stages or normal condition for early and accurate diagnosis.

➢ *Proposed System Description*

The proposed system for early Alzheimer's disease detection follows a structured processing pipeline comprising several sequential stages. The input medical image set, consisting of brain MRI scans, is first fed into the framework for transformation. The images then undergo processing through an ACF, which removes unwanted noise while preserving the core anatomical structures necessary for identifying early-stage AD. The processed images are subsequently divided into training and testing subsets.

After preprocessing, features are extracted and a classifier is built using a hybrid DBN–ViT architecture. In this architecture, the DBN learns structured feature representations, while the Vision Transformer captures local patterns and long-range relationships through its attention mechanism. The model parameters are further optimized using ChOA, which improves both classification accuracy and training speed. Finally, the optimized DBN–ViT model produces a prediction that classifies each image into a specific Alzheimer's disease stage or a normal cognitive condition.

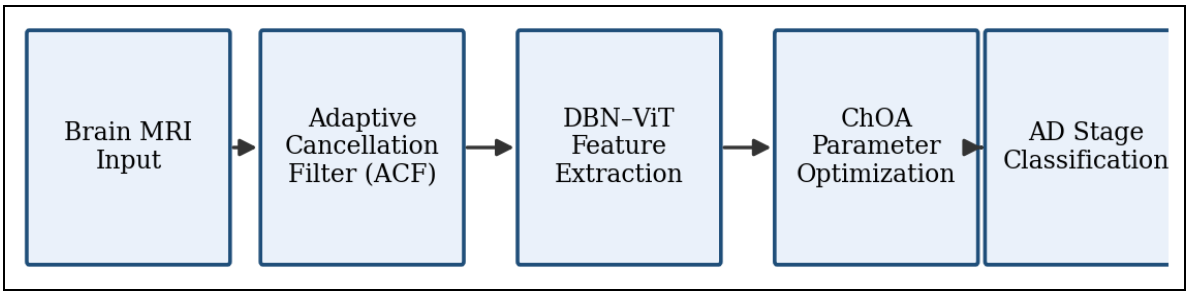

Fig 1 Block Diagram of the Proposed System

II. PROPOSED SYSTEM MODELLING

➢ *Preprocessing*

In AD research, EEG and MEG signals are commonly used to detect low-frequency brain activity associated with cognitive impairment. These signals are frequently distorted by artefacts and ambient noise, which necessitates preprocessing. An ACF is therefore employed to reduce correlated noise while preserving AD-related neural information.

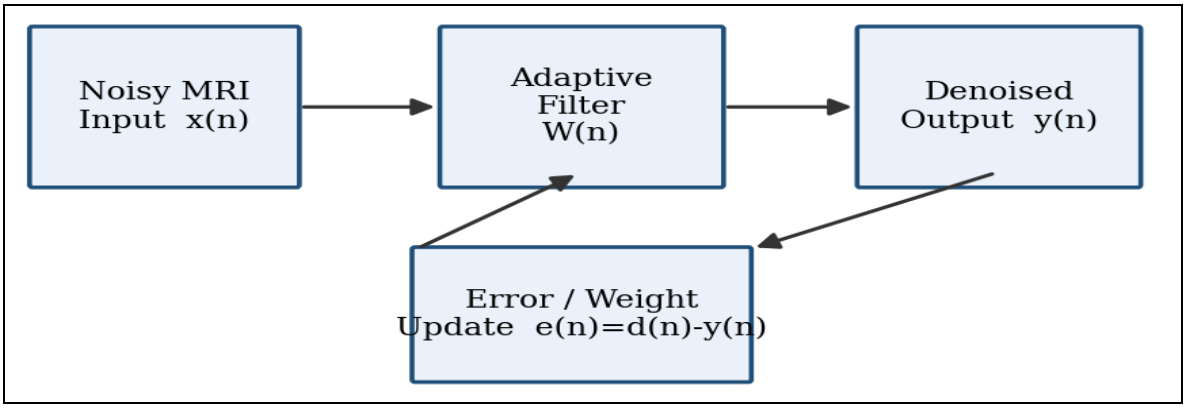

Fig 2 Block Diagram of the ACF

Assuming the recorded EEG/MEG signal (primary input d) arises from brain activity s and additive noise n_0, the relationship is expressed as:

ISSN No:-2456-2165 https://doi.org/10.38124/ijisrt/26jul1280

$$d = s + n_0 \quad (1)$$

The reference sensor simultaneously records a noise-dominated signal that is correlated with the noise in the primary signal, possibly originating from an external electromagnetic field:

$$x = n_1 \quad (2)$$

Where n_0 and n_1 denote the correlated noise sources that the filtering process separates. The adaptive filter uses the reference input to eliminate the noise component from the primary EEG/MEG signal, producing an output:

$$y = W^T x \quad (3)$$

The coefficient vector of the adaptive filter (W) is iteratively updated based on an error cost function, allowing a cleaner neural signal to be obtained from the primary signal (d) by removing the estimated noise (y), which supports subsequent AD assessment.

In AD patients, EEG and MEG recordings commonly exhibit impulsive, non-Gaussian noise arising from muscle movement, electrode interference, and abnormal neuronal activity. To capture this behaviour during preprocessing, α-stable distributions are used. These distributions do not have a closed-form probability density function; instead, they are defined through their characteristic function:

$$\varphi(t) = \exp\{j\delta t - \gamma|t|^\alpha [1 + j\beta \cdot \text{sign}(t) \cdot \omega(t,\alpha)]\} \quad (4)$$

The auxiliary function ω(t, α) is given by:

$$\omega(t,\alpha) = \tan(\pi\alpha/2), \text{ for } \alpha \neq 1; \ (2/\pi)\cdot\log|t|, \text{ for } \alpha = 1 \quad (5)$$

The sign function is defined as:

$$\text{sign}(t) = 1 \text{ for } t > 0; \ 0 \text{ for } t = 0; \ -1 \text{ for } t < 0 \quad (6)$$

Through this process, correlated and impulsive noise is reduced while AD-related neural information is preserved, thereby improving the quality of EEG/MEG recordings and enabling more accurate evaluation of individuals with AD.

➢ *Data Partitioning*

Data partitioning is essential for building a reliable AD detection model. The EEG, MEG, or neuroimaging data are divided into training, validation, and testing subsets. The training set allows the model to learn neural patterns associated with cognitive decline in AD. The validation set is used to tune model parameters and reduce the risk of overfitting. Finally, the model is evaluated on the testing set, providing an unbiased assessment of its ability to detect early signs of AD.

III. DBN–VIT

The first stage of the proposed detection pipeline is the ViT, which analyses brain images such as MRI or PET scans to extract global and local neurodegenerative features. An input brain image X ∈ R^(H×W×C) is divided into fixed-size, non-overlapping patches of size P×P, yielding a total number of patches:

$$N = (H/P) \times (W/P) \quad (7)$$

Each patch $x_i \in R^{(P^2 \cdot C)}$ is flattened and linearly embedded as:

$$z_i = x_i W_e + b_e \quad (8)$$

Patch embeddings are supplemented with positional embeddings to preserve anatomical and spatial information about the brain:

$$z_i^{(0)} = z_i + p_i \quad (9)$$

The resulting embeddings pass through several transformer encoder layers, where the self-attention mechanism allows brain regions to interact globally. The self-attention operation is defined as:

$$\text{Attention}(Q,K,V) = \text{softmax}(QK^T/\sqrt{d_k})\cdot V \quad (10)$$

This mechanism enables long-range dependencies and AD biomarkers, such as cortical degeneration and hippocampal atrophy, to be efficiently captured by the ViT.

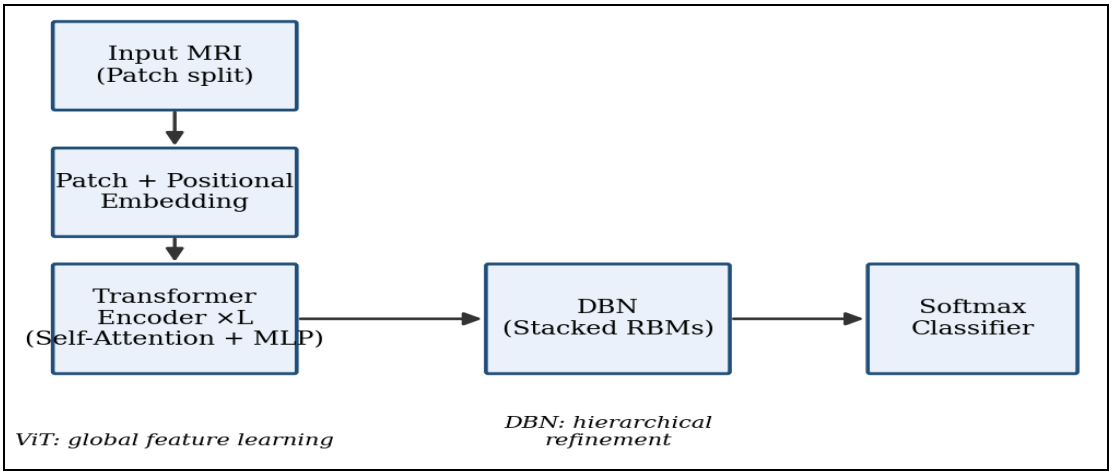

Fig 3 DBN–ViT Architecture

ISSN No:-2456-2165 https://doi.org/10.38124/ijisrt/26jul1280

The representations learned by the ViT are passed to the DBN for further refinement. The DBN learns hierarchical representations in an unsupervised, layer-by-layer fashion using stacked Restricted Boltzmann Machines (RBMs). The relationship between each RBM's visible layer (v) and hidden layer (h) is modelled using the energy function:

$$E(v,h,\theta) = -\Sigma_{i,j} w_{ij}v_ih_j - \Sigma_i a_iv_i - \Sigma_j b_jh_j \quad (11)$$

This energy function defines the joint probability distribution of the visible and hidden units:

$$P(v,h,\theta) = (1/Z(\theta))\cdot\exp(-E(v,h,\theta)) \quad (12)$$

Where $Z(\theta)$ denotes the partition function. Latent AD patterns are captured through the conditional probability of hidden unit activation:

$$P(h_j = 1 \mid v) = \sigma(b_j + \Sigma_i v_iw_{ij}) \quad (13)$$

Using the sigmoid activation function:

$$\sigma(x) = 1 / (1 + e^{\wedge}(-x)) \quad (14)$$

By stacking several RBMs, the DBN refines the ViT-derived features into compact, discriminative representations that efficiently model disease progression.

The hybrid ViT–DBN framework thus combines the DBN's hierarchical probabilistic learning with the ViT's global attention capacity. The ViT successfully captures long-range spatial dependencies between AD-affected brain regions, while the DBN further refines these features into deeper, disease-specific representations. This hybrid approach improves both classification accuracy and robustness, particularly for early AD detection.

➢ *Chimp Optimization Algorithm (ChOA)*

Inspired by chimpanzee hunting behaviour, ChOA is used to improve AD detection performance. The search process is guided by four roles: the attacker identifies the most informative features, the driver directs the search toward promising solutions, the chaser investigates candidate features, and the barrier restricts irrelevant ones. This coordinated process balances exploration and exploitation to maximize feature selection and overall model performance.

A mathematical model of chimpanzee enclosing and pursuit behaviour is used for AD detection. The distance between a candidate solution and the optimal solution is defined as:

$$D = |C\cdot X\_best(t) - m\cdot X\_candidate(t)| \quad (15)$$

And the candidate solution is updated as:

$$X\_candidate(t+1) = X\_best(t) - a\cdot D \quad (16)$$

Where X_candidate is the current candidate solution, X_best is the optimal solution, and t is the current iteration. The coefficients a, m, and c, which govern exploration and exploitation, are computed using random and chaotic factors:

$$a = 2\cdot f\cdot r_1 - f \quad (17)$$

$$m = \text{chaotic value}, \quad c = 2\cdot r_2 \quad (18)$$

Here, r_1 and r_2 are random vectors in [0, 1], f is a convergence factor that decreases from 2.5 to 0 and controls the step size, m introduces chaotic randomness, and c controls the influence of the optimal solution.

Following population initialization, the four best solutions — attacker, barrier, chaser, and driver — are selected based on classification performance. The positions of the remaining candidate solutions are then updated around these four solutions as follows:

$$X_1 = X\_attacker - a_1\cdot|C_1\cdot X\_attacker - m_1\cdot X| \quad (19)$$

$$X_2 = X\_barrier - a_2\cdot|C_2\cdot X\_barrier - m_2\cdot X| \quad (20)$$

$$X_3 = X\_chaser - a_3\cdot|C_3\cdot X\_chaser - m_3\cdot X| \quad (21)$$

$$X_4 = X\_driver - a_4\cdot|C_4\cdot X\_driver - m_4\cdot X| \quad (22)$$

The final candidate solution is obtained by averaging these four updated positions:

$$X(t+1) = (X_1 + X_2 + X_3 + X_4) / 4 \quad (23)$$

By balancing the exploration of new feature combinations with the exploitation of high-performing solutions, ChOA improves the precision, resilience, and reliability of the AD detection model.

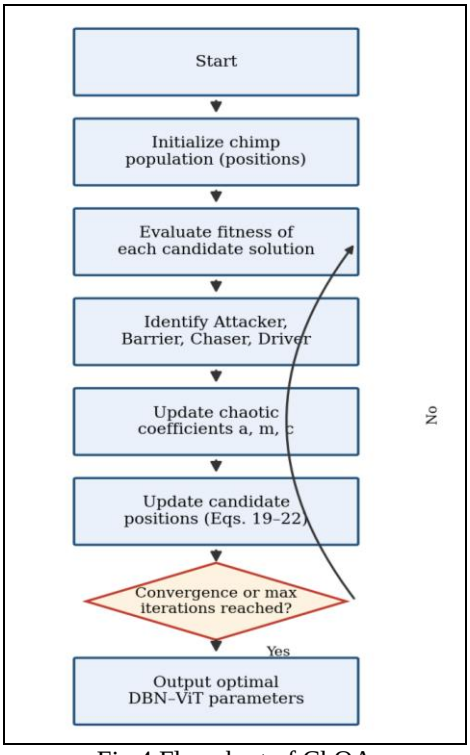

Fig 4 Flowchart of ChOA

ISSN No:-2456-2165 https://doi.org/10.38124/ijisrt/26jul1280

IV. RESULTS AND DISCUSSION

This section presents the findings obtained from experimentation using the DBN–ViT model for dementia classification from MRI brain scans. The effectiveness of each stage of the pipeline — preprocessing, feature extraction, and classification — is assessed both visually and quantitatively.

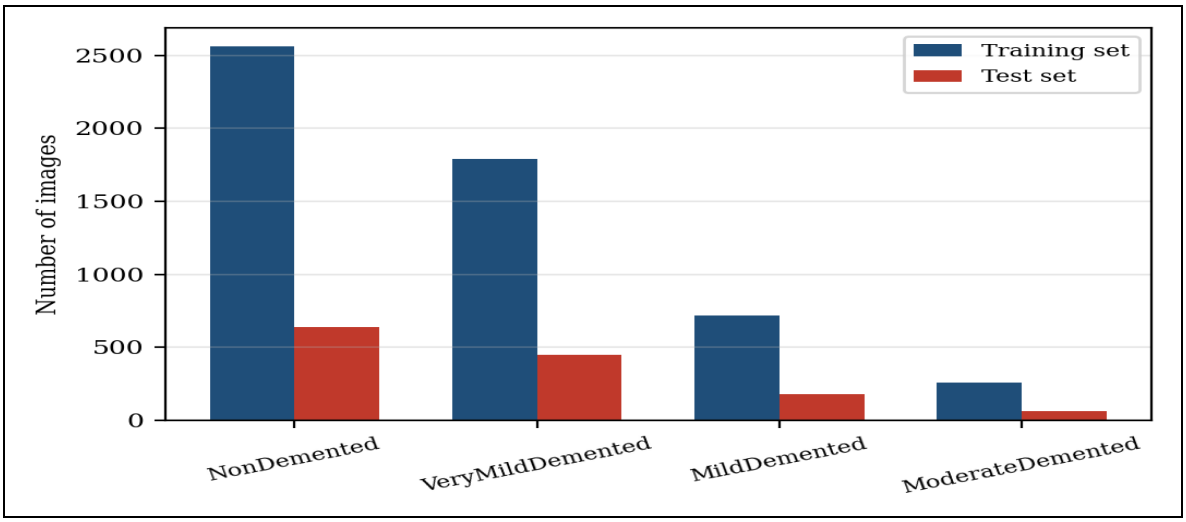

Fig 5 Train vs. Test Dataset Distribution

Figure 5 shows the distribution of images across four dementia-related categories, comparing the number of images in the training and test sets. All four categories contain more images in the training set than in the test set, with the NonDemented category containing the largest number of images.

Table 1 Performance Evaluation Metrics of the Proposed Model

Performance Metric	Value
Accuracy	95%
Precision	95%
Recall	95%
F1-score	95%

Table 1 summarizes the predictive performance of the proposed model using standard evaluation metrics. The model achieves 95% accuracy, precision, recall, and F1-score, indicating consistently high and stable classification performance.

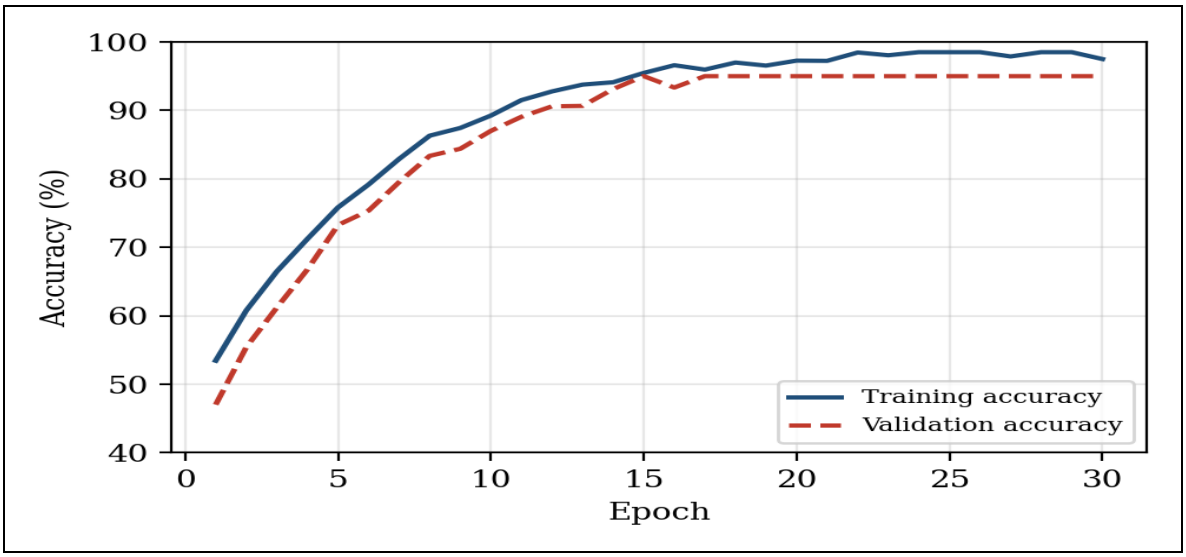

Fig 6 Model Accuracy Over Training Epochs

Figure 6 shows the training and validation accuracy across epochs. The steady increase in both curves indicates effective learning and convergence, and their close alignment reflects good generalization.

ISSN No:-2456-2165 https://doi.org/10.38124/ijisrt/26jul1280

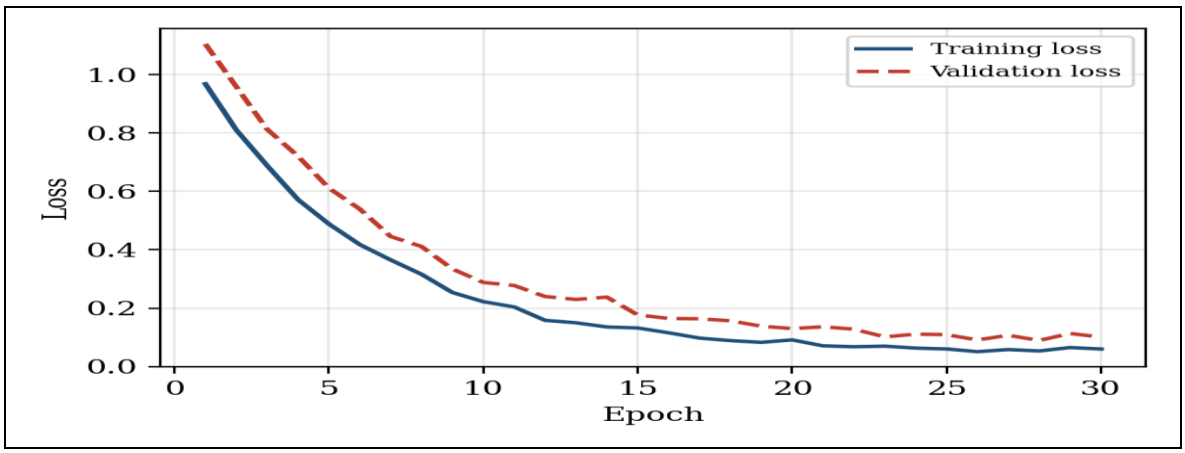

Fig 7 Model Loss Over Training Epochs

Figure 7 shows the training and validation loss decreasing across epochs, with both curves dropping rapidly during early training as the model converges. The close similarity between the two loss curves indicates a low degree of overfitting.

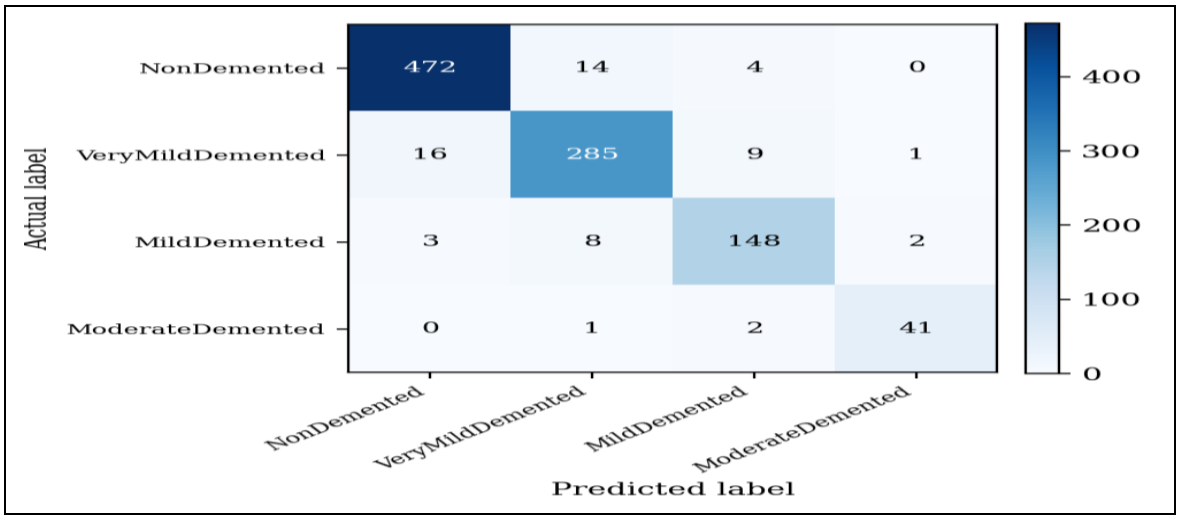

Fig 8 Confusion Matrix for Dementia Classification

Figure 8 presents the confusion matrix comparing actual and predicted class labels. The diagonal values are relatively high across all dementia stages, indicating correct classification in most cases, with minor misclassifications occurring mainly between adjacent stages of dementia.

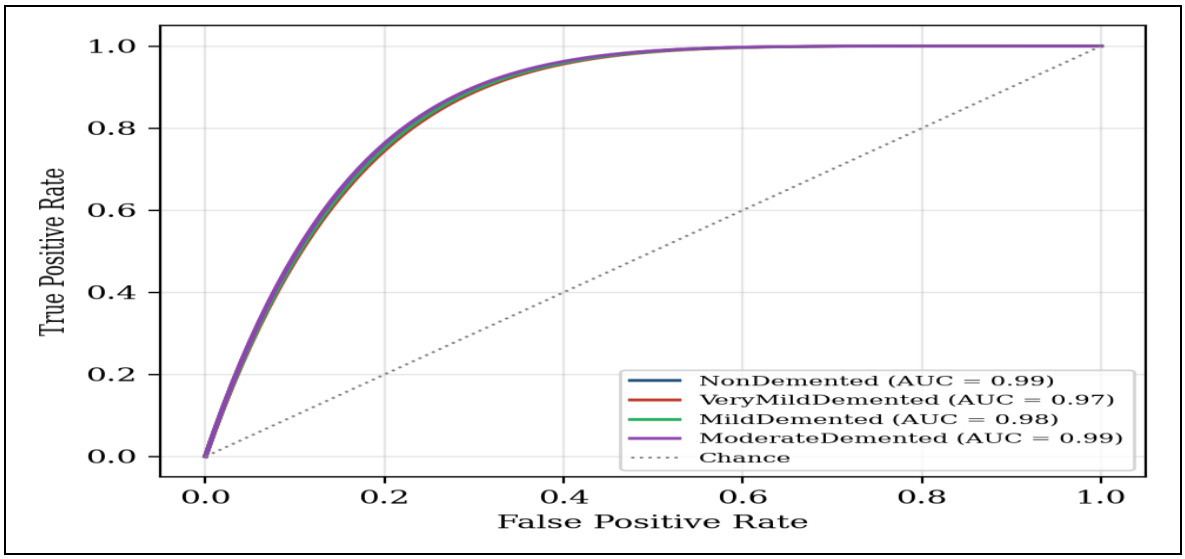

Fig 9 Multiclass ROC Curve for Dementia Classification

ISSN No:-2456-2165 https://doi.org/10.38124/ijisrt/26jul1280

Figure 9 shows ROC curves for each dementia class with high AUC values, indicating strong separation performance across all classes and substantially better performance than random guessing.

Table 2 Comparison of Model Accuracy

Method	Accuracy
Decision Tree [12]	89%
CNN [13]	92%
Proposed	95%

Table 2 compares the accuracy of the Decision Tree (DT), Convolutional Neural Network (CNN), and the proposed model. The proposed model achieves the highest accuracy at 95%, outperforming both baseline methods.

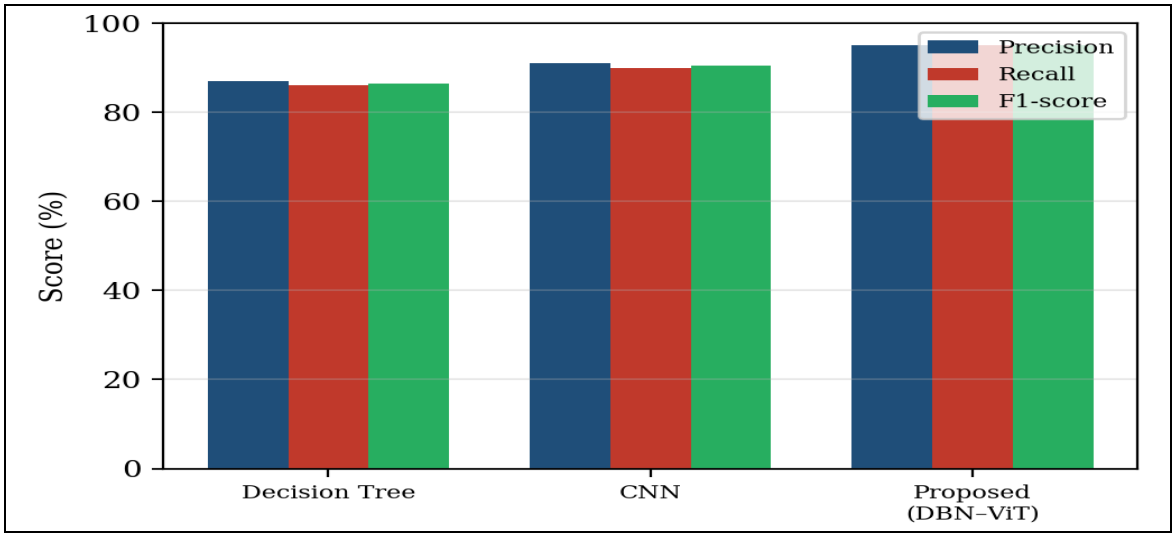

Fig 10 Comparison of Precision, Recall, and F1-Score Across Methods

Figure 10 compares precision, recall, and F1-score across the evaluated methods. The proposed model achieves the highest scores across all three metrics, demonstrating superior and more consistent classification performance relative to the baseline methods.

V. CONCLUSION

This study demonstrates that the proposed DBN–ViT model performs well on multiclass dementia classification from brain MRI images. With an accuracy of 95% and precision, recall, and F1-score all reaching 95%, the model produces classification results that are highly dependable and consistent. Preprocessing steps such as resizing, grayscale conversion, and ACF-based enhancement improve image clarity and support efficient feature extraction. The closely aligned training and validation loss curves confirm minimal overfitting, while the corresponding accuracy curves demonstrate steady convergence. The comparative analysis further confirms that the proposed model outperforms CNN (92%) and Decision Tree (89%) techniques, supporting its effectiveness for precise dementia stage identification.

REFERENCES

[1]. H. A. Helaly, M. Badawy, and A. Y. Haikal, "Deep learning approach for early detection of Alzheimer's disease," Cognitive Computation, vol. 14, no. 5, pp. 1711–1727, 2022.

[2]. S. Liu, A. V. Masurkar, H. Rusinek, J. Chen, B. Zhang, W. Zhu, C. Fernandez-Granda, and N. Razavian, "Generalizable deep learning model for early Alzheimer's disease detection from structural MRIs," Scientific Reports, vol. 12, no. 1, p. 17106, 2022.

[3]. A. G. Vrahatis, K. Skolariki, M. G. Krokidis, K. Lazaros, T. P. Exarchos, and P. Vlamos, "Revolutionizing the early detection of Alzheimer's disease through non-invasive biomarkers: The role of artificial intelligence and deep learning," Sensors, vol. 23, no. 9, p. 4184, 2023.

[4]. J. Venugopalan, L. Tong, H. R. Hassanzadeh, and M. D. Wang, "Multimodal deep learning models for early detection of Alzheimer's disease stage," Scientific Reports, vol. 11, no. 1, p. 3254, 2021.

[5]. B. Khagi, K. H. Lee, K. Y. Choi, J. J. Lee, G. R. Kwon, and H. D. Yang, "VBM-based Alzheimer's disease detection from the region of interest of T1 MRI with supportive Gaussian smoothing and a Bayesian regularized neural network," Appl. Sci., vol. 11, no. 13, p. 6175, 2021.

[6]. A. B. Tufail, Y. K. Ma, M. K. A. Kaabar, A. U. Rehman, R. Khan, and O. Cheikhrouhou, "Classification of initial stages of Alzheimer's disease through PET neuroimaging modality and deep learning: Quantifying the impact of image filtering approaches," Mathematics, vol. 9, no. 23, p. 3101, 2021.

ISSN No:-2456-2165 https://doi.org/10.38124/ijisrt/26jul1280

[7]. K. AlSharabi, Y. Bin Salamah, A. M. Abdurraqeeb, M. Aljalal, and F. A. Alturki, "EEG signal processing for Alzheimer's disorders using discrete wavelet transform and machine learning approaches," IEEE Access, vol. 10, pp. 89781–89797, 2022.
[8]. M. J. Oliveira, P. Ribeiro, and P. M. Rodrigues, "Machine learning in Alzheimer's disease diagnosis," Bioengineering, vol. 11, p. 1153, 2024.
[9]. G. Pahuja and T. N. Nagabhushan, "A novel GA-ELM approach for Parkinson's disease detection using brain structural T1-weighted MRI data," in Proc. 2nd Int. Conf. Cognitive Computing and Information Processing (CCIP), IEEE, 2016.
[10]. A. Elaraby, W. Hamdy, and M. Alruwaili, "Optimization of deep learning model for plant disease detection using particle swarm optimizer," Computers, Materials & Continua, vol. 71, no. 2, 2022.
[11]. J. Wu, R. Tao, P. Zhao, N. F. Martin, and N. Hovakimyan, "Optimizing nitrogen management with deep reinforcement learning and crop simulations," in Proc. IEEE/CVF Conf. Computer Vision and Pattern Recognition, 2022.
[12]. M. Odusami, R. Maskeliūnas, R. Damaševičius, and T. Krilavičius, "Analysis of features of Alzheimer's disease: Detection of early stage from functional brain changes in magnetic resonance images using a fine-tuned ResNet18 network," Diagnostics, vol. 11, no. 6, p. 1071, 2021.